Electrostatic Focusing of Electrospun Polymer(PEO) Nanofibers

Rudolf Kyselica[a], Eniko T. Enikov[1a], Peter Polyvas,[a], Rein Anton[b]

[a] *Aerospace & Mechanical Engineering, The University of Arizona, Tucson, AZ 85721, USA*
[b] *Department of Surgery, The University of Arizona, Tucson, AZ 85721, USA*

Abstract

Polymer nanofibers have a specific set of material properties that are favorable for many applications in biomedical engineering (scaffolds, stents or tissues engineering). In this article, influence of the electrostatic field distribution on the fiber deposition pattern is examined. The electrode pair used in the study is part of a lineal quadrupole trap used in ion trapping experiments. The impact of the bias potential on the nanofiber collection patterns and the electrospinning process is examined through a series of experiments and finite-element analysis of the resulting field distribution. A set of optimal amplitudes of the steering electric field components is also reported.

Keywords: Electrospinning, Electrostatic Focusing, Paul Trap, Nanofiber

1. Introduction

Electrospinning is a versatile and inexpensive fiber extrusion technique capable of producing nanometer-sized fibers [1, 2]. Since its development in early 20th century, it has been improved significantly in terms of instrument design [3] and ability to extrude a wide variety of polymers . However, the electrospinning process parameters, which significantly influence the produced nanofiber, are still not fully understood. Alignment and orientation of the fiber is achieved mostly mechanically trough dynamic or specially shaped collector electrode.

[1] Corresponding author.
Email address: enikov@email.arizona.edu

The simplest electrospinning apparatus contains a liquid polymer (solution or melt) container with a blunt needle serving as a nozzle, a DC high voltage source connected to it, and a lower potential collecting electrode. By applying DC high voltage to this nozzle, particles of the polymer solution become charged with the electric charge of the same polarity, what creates repulsive Coulomb forces in between them. These forces are growing with applied voltage and create a bubble-like droplet at the tip of the nozzle, which will with further increase of voltage transform into a Taylor cone. If applied voltage reaches a threshold value and repulsive forces overcome the surface tension, a thin jet of fluid polymer is created from the tip of the Tayler cone. After the jet is created, it still is under the influence of repulsive Coulomb forces between its particles. This very quickly leads to a bending instability and the jet/fiber starts spiraling (hence electrospinning) on its way to the collector. It was shown[1], that multiple orders of bending instability on top of each other occure as the fiber propagates to the collector. The electrospun fiber under bending instability of the first three orders can be seen in Fig.1

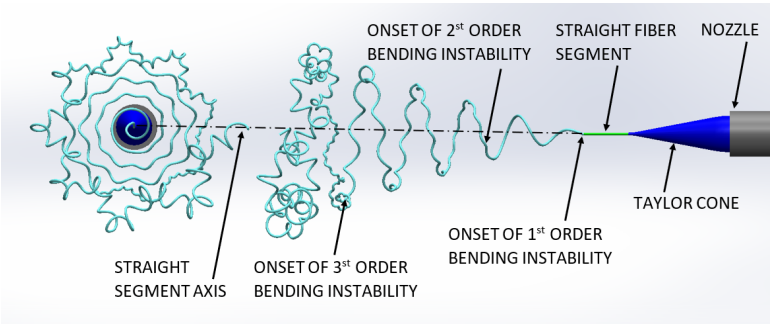

Fig. 1. Ilustration of a polymer jet creation in electrospinning process folowed by first three succesive electric charge driven bending instabilities.

Because of the drag from the potential difference between a charged fiber and a low potential collector and because of the solvent evaporation, liquid polymer jet stretches, decreases its thickness and solidifies. Because of occurrence of previously described bending instability, if left without any additional

focusing, electrospinning would lead to a collection of highly buckled strains of polymer nanofiber, with no orientation or alignment on micro- or macro-scopic scale. This has been widely investigated and various solutions were introduced [4, 5, 6, 7, 8, 9]. Mostly dynamic collector, spinning mandrel/ drum, is used, which at optimal angular velocity straightens and winds the fiber. Often collection in between multiple grounded object, or on the flowing liquid is also used. In summation, all the developed techniques require complex collection mechanisms and consequently a fiber transfer from the collector to an area of interest. Electrostatic and electrodynamic stearing of the electrospun nanofiber have also been implemented [9, 10, 11, 12, 13], and focusing capabilities of external electric field were shown in size reduction of fiber deposit. Also, straightening of the fiber in micro-scale in combination of use of external electric field and dynamic collector electrode were shown. However, the parameters of the steering device are not yet fully understood, and neither is the influence of the auxiliary electrodes on the fiber extrusion itself.

To mitigate impact of the internal Coulomb forces and avoid the use of indirect fiber collection, long-term objective of this research is to find an closed-loop electrodynamic control method of the electrospun polymer nanofiber. The premise of the approach is that trapping the fiber on a quasi-periodic trajectory could stabilize the unstable buckling modes resulting in a straight-line deposition. A possible feedback signal can be obtained from current sensors attached to a segmented collector electrode. As a controller, adjusted Paul linear quadrupole trap [14] with hyperbolically shaped electrodes will be used. This paper examines the electric field distribution within such trap from the point of view of fiber propagation and extrusion. The quadrupole trap is in our case is expanded by the axial coordinate (z-axis) dependent term, representing the influence of the trap on the fiber in the axial (propagation) direction, and is described by equation Eqn.1.

$$\Phi = \frac{1}{2}\left(U_{DC} + U_{AC}\cos\left(\omega\, t\right)\right)\left(\alpha x^2 - \beta y^2\right) - \gamma\, z \tag{1}$$

where α, β and γ are coefficients corresponding to the electrode geometry. Linear electrostatic traps typically operate in two-directions using a alternating fields. In a given cycle, one of the directions has confining action, while the transversal direction is anti-confining. By choosing a frequency that matches the motion of the fiber, it is possible to constrain it to a quasi-periodic trajectory by alternating the confining and anti-confining directions. This is illustrated by the electric field in the trap (x - confining, y - anti-confining) in Eqn.2 and 3, respectively. The electric field along the z-axis of the device is described by Eqn.4 and is not intended to confine the fiber.

$$E_x = -\frac{\partial \Phi}{\partial x} = -\alpha \, \left(U_{DC} + U_{AC} \, \cos\left(\omega \, t\right)\right) \, x \tag{2}$$

$$E_y = -\frac{\partial \Phi}{\partial y} = \beta \, \left(U_{DC} + U_{AC} \, \cos\left(\omega \, t\right)\right) \, y \tag{3}$$

$$E_z = -\frac{\partial \Phi}{\partial z} = \gamma \tag{4}$$

To satisfy the Laplace equation, $(\Delta \, \Phi \, = \, 0)$ one arrives at $\alpha \, = \, \beta$, which should hold under the assumption that the net charge on the fiber is small compared to the charges on the confining electrodes. Then external electric forces on a fiber segment with an electric charge of Q are as given in Eqn.5, Eqn.6 and Eqn.7.

$$F_x = -\alpha \, Q \, \left(U_{DC} + U_{AC} \, \cos\left(\omega \, t\right)\right) \, x \tag{5}$$

$$F_y = \alpha \, Q \, \left(U_{DC} + U_{AC} \, \cos\left(\omega \, t\right)\right) \, y \tag{6}$$

$$F_z = \gamma \, Q \tag{7}$$

Equations of motion for a charged particle in linear quadrupole trap are known as Mathieu equations [15]. Their analytical solutions and stability regions are known [16] in terms of frequency and amplitude of the applied har-

monic forcing function. In our application, strings of charged particles are propagating trough the trap. This not only introduces additional non-linear terms in equations of motion (mechanical forces, internal Coulomb forces, Stokes drag force), but also significantly increases the number of degrees of freedom (based on fiber discretization). Discretized fiber segment, as we assume it, is shown in Fig.2, and a corresponding system of equations of motion is shown below in Eqn. 8

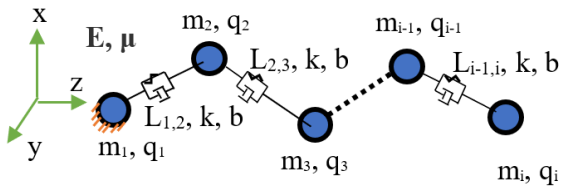

Fig. 2. Spring-mass model of the discretized fiber.

$$
\begin{aligned}
&m\,\ddot{x}_{j,i} + c\,\dot{x}_{j,i} + b\,\frac{d\,L_{i,i-1}}{d\,t}\,\frac{(x_{j,i}-x_{j,i-1})}{L_{i,i-1}} - b\,\frac{d\,L_{i,i+1}}{d\,t}\,\frac{(x_{j,i}-x_{j,i+1})}{L_{i,i+1}} + \ldots \\
&\ldots + k\,(x_{j,i}-x_{j,i-1})\left(1-\frac{L}{L_{i,i-1}}\right) - k\,(x_{j,i+1}-x_{j,i})\left(1-\frac{L}{L_{i,i+1}}\right) - \ldots \\
&\ldots - \sum_{k=1}^{n}\left(\frac{k_e\,q^2}{L_{i,k}^3}\,(x_{j,i}-x_{j,k})\right) + F_j = 0
\end{aligned}
\tag{8}
$$

In Eqn.8, $j=[1,3]$ $,i=[1,n]$ $,i,j\in N$. n is the number of beeds to which the fiber is discretized, and j represents axis in cartesian system.$x_{j,i}$ is then the j-th component of a position vector $\bar{x}$ of the i-th beed. $L_{i,i-1}$ is a length of the fiber segment between i-th and (i-1)-th beed and is expressed in Eqn.9

$$
L_{i,i-1} = \sqrt{\sum_{j=1}^{3}\left(x_{j,i}-x_{j,i-1}\right)^2} \tag{9}
$$

Analytical solution of this system of differential equations becomes not practically feasible, and so the system stability regions need to be found using nu-

merical and experimental studies. As an initial step discussed in this article, we examine the trap under static condition, where $U_{AC} = 0$ and $\beta U_{DC} \neq 0$. Under such conditions, we anticipate the fiber to be constrained in a single plane. Important quantities such as electric field distribution and electric field gradient, βU_{DC}, can then be obtained from FEA analysis corresponding to such planar configuration. Subsequently, replicating these fields in the transversal direction will allow the implementation of a full quadrupole trap. To estimate the range of amplitudes of the forcing function, we introduced electrostatic focusing electrodes to the classical electrospinning device. Using large lateral fields might seem advantageous as it increases the control authority of the electrodes, however it also distorts the axial field as will become apparent in the subsequent sections of this paper. Therefore the main objectives of this study is to establish values of electric field suitable for electrodynamic forcing amplitudes in electrodynamic fiber control.

2. Materials and Methods

2.1. Materials

A polyethylene oxide (PEO) solution of 5 wt% ,7.5 wt% and 10 wt% in DI (Deionized) water was prepared by dissolving corresponding amount of PEO powder in 80° C water while stirring the solution. Beaker was than sealed to prevent water loss and kept at 80°C, while constant stirring at 120 RPM for a minimum of 8 hours, or until uniform solution density was obtained.

2.2. Electrospinning experiments

Electrospinning device used for experiments consists of acrylic walls as an enclosure and 3D printed PLA (Polylactic Acid) components as rails, nozzle and electrode holders. The use of conductive materials was limited to just nozzle and auxiliary electrodes, to eliminate electrical breakdowns between the components, and to minimize a deformation of the electric field distribution created by the set of auxiliary electrodes. Because of used materials and sufficient spacing

between conductive components of the device, it was operated in the air at room temperature and normal pressure. Minimal distance between charged electrode and a ground electrode was however larger than Paschen curve indicates to be-safe, as humidity accumulation in the device while electrospinning influences the air breakdown voltage. This minimal distance between conductive components of potential difference U=11kV was found to be about d=12mm. As a collector electrode, ITO (Indium-Tin-Oxide) coated glass slides 50x75x0.7mm (CB-50IN-S207 from Delta technologies) were used. The coated surface of 5-15 (connected from the back side of the slide to the ground), was used for the fiber collection. Low resistance of the collector electrode is important for charge dissipation from the collected fiber, to prevent repulsion between collected and incoming fiber. Focusing electrodes were flat 100x10x1mm copper plates, and for nozzle, stainless steel 1.0" long blunt dispensing tips from CML Supply were used.

While electrospinning process was initiated, the collector electrode was covered by a thin plastic sheet with grounded Cu tape of size of the collector electrode, that served as a temporary collector and was removed when all the testing parameters were adjusted. It was later placed back in shielding position after sufficient fiber sample was collected on the collector slide.

Processing of the fiber deposits was done in MATLAB, where pictures of the collector slides with reference square were input. Figures changed to binary figures were then used to find a total area of deposition and deposition region aspect ratio.

To generate a set of parameters for experiments, Box-Behnken design was used [17]. This is a class of incomplete three-level factorial designs useful for decrease of experimental redundancy. In this experimental arrangement with eight chosen parameters (described in following section)this lead to a total of 120 experiments.

2.3. Simulations

FEA (finite-element analysis) analysis of the electric field inside the device was performed in COMSOL Multiphysics 5.2, with use of material properties from builtin material library. Environment - air, nozzle and collector - soft iron, focusing electrodes - copper. Sizes and distances between components were modelled based on the components used in experiments described in previous subsection.

3. Electrostatic Focusing

The simplest arrangement of confining electrodes is a pair of flat, rectangular electrodes with DC voltage of the same polarity as the nozzle voltage. From Earnshaws theorem it is known, that charged particles, in this case a string of charged particles, cannot be kept in static equilibrium solely by static electric field. However, to partially constrain the fiber in space and influence it‘s deposition on the collector (in macroscopic scale), it is sufficient to use electrostatic field. As the fiber propagates from the nozzle to a collector, it passes through the region between the focusing electrodes and so through the electric field created by these electrodes. As the fiber and confining electrodes have the same charge polarity, the fiber is repelled away from the surface of these electrodes. This results in confinement of the fiber movement and therefore also the fiber deposition area on the collector. Different electric field configurations inside the device were achieved by varying the position of focusing electrodes along the device axis (EC), their separation (EE) and applied voltage onto these electrodes (EV). Different electric field inside of the electrospinning device introduces different external Coulomb forces applied to the fiber, what leads to different fiber deposition pattern on the grounded collector electrode. Besides the focusing electrodes parameters, impact of eight electrospinning device parameters the fiber properties was investigated. These parameters are: Nozzle diameter (N), nozzle voltage (NV) and its distance from the collector (NC), flow rate (FR, also called feed rate) of the polymer solution and the PEO (poly ethylene oxide)

concentration in this water-based solution (CC).The electrospinning device is shown in Fig.3 below, and its schematic view marked parameters is shown in Fig.4. The most influential electrospinning device parameters are described in following section.

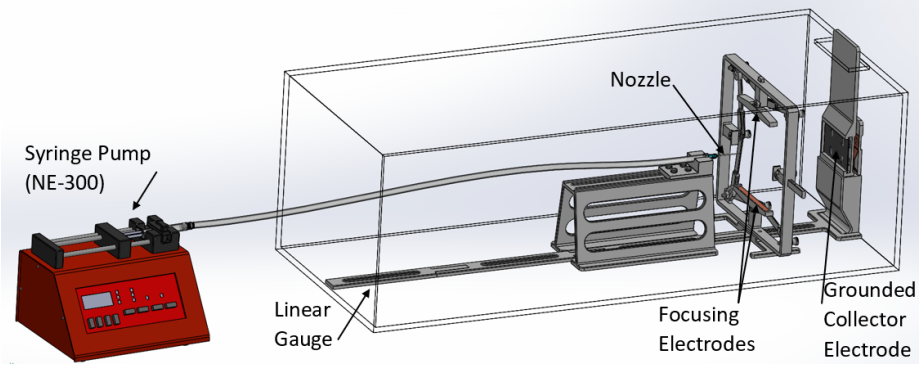

Fig. 3. Electrospinning device as described in this article, with its components.

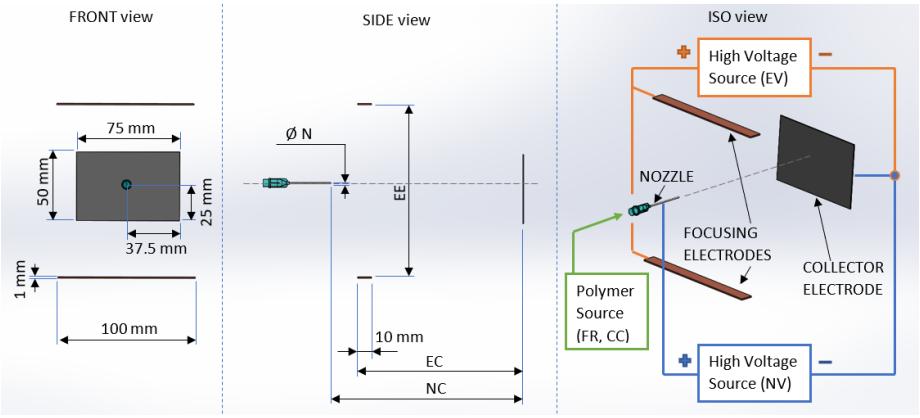

Fig. 4. Electrospinning device with marked parameters. These parameters are described further in this article.

4. Electrospinning Device Parameters

Nozzle Voltage (NV). After the threshold nozzle voltage is reached and a polymer jet is created, we observed, that the nozzle voltage can be reduced about 10%-15%, without stopping the fiber from spinning. Generally, lower nozzle voltages lead to finer (lower diameter) fiber which dries faster. Increase in nozzle voltage leads to a more mass being pushed into a jet and so either thicker fiber or creation of multiple fibers are created. Neither of these cases are desirable for both electrostatic and electrodynamic fiber focusing. The thicker fiber might not have enough time to dry on its path to a collector and would deposit wet. For electrostatic or electrodynamic focusing, multiple fiber creation is not desirable. These charged fibers are distorting the electric field created inside the device and are influencing the other fibers, as they repel each other. At the same time, we were not able to find any combination of parameters, that would lead to a specific number of created fibers.

Solution Concentration (CC). In this study three different concentrations of poly ethylene oxide (PEO) in water were investigated. 5%, 7.5%, and 10%. Concentration of a polymer solution influences the stretchability and material integrity of the fiber trough viscosity resp. surface tension. In general, if the concentration is too low, it leads to electrospraying where non-fibrous elements are collected. At optimal concentration, fiber after extrusion is evenly stretched by internal Coulomb forces and smooth fiber is obtained. With further increase in concentration, premature drying of the polymeric solution at the tip of the nozzle might ocure, and defective (mostly beeded) fiber is collected [18]. From the performed set of experiments, 5% solution was found to provide the best results.

Flow rate (FR). Significance of flow rate of the polymer solution in the needle and its impact on the fiber parameters is not well understood. Some researchers found minimal impact across the tested range [19] and others found significant impact of flow rate on the fiber properties [20]. Our experiments support find-

ings of the later article. The smoothest fiber, and a consistent fiber production were achieved with minimal flow rate, sufficient to provide consistent polymer solution supply to the Taylor cone and to the electrospun fiber. With lower flow rate, electrospinning was stopped and restarted after accumulation of sufficient solution in the needle. With increasing flow rate above the optimal level, fiber thickness was first increased, polymer solution droplet formed at the tip of the nozzle and multiple fibers were often created. This is shown in Fig.5

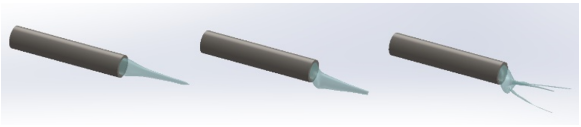

Fig. 5. Tayler cone deformation due to higher than optimal flow rate.

Nozzle to Collector Electrode Distance (NC). There are tradeoffs in nozzle to collector distance. With increase in this distance, fiber needs to travel longer distance before it deposits on the collector. This gives it more time to undergo higher orders of bending instability, resulting in more buckled fiber. Decreasing the nozzle to collector distance is reducing the fiber flight time and so the drying time. If this distance is too short, wet fiber deposition will occur. Optimal combinations of these most influential device parameters in terms of stability of fiber extrusion are shown in the following section.

5. Fiber Extrusion Regimes

From the above described parameters, nozzle to collector distance (NC), confining electrode voltage (EV), electrode to collector distance (EC) and nozzle voltage (NV) were found to be the most influential in terms of stable fiber extrusion. Stable extrusion was defined as a continuous production of a single nanofiber, that is deposited dry. Varying these most influential parameters, different fiber extrusion regimes were found. These three regimes, for three

different nozzle-to-collector distances, are shown in Fig.6, where the stable extrusion regime is marked in yellow. The bottom surface of this region shows the threshold nozzle voltage for given combination of electrospinning parameters. There is no fiber extrusion below this surface. The upper boundary surface shows at what nozzle voltage the device starts spinning multiple fibers or thicker fibers that deposit wet. Above this surface, device operates in the unstable fiber extrusion regime. It can be seen, that for the lowest nozzle to collector distance of NC=50 mm, the stable fiber extrusion regime is very limited. Reducing this distance even further would result in always wet or multiple wet fibers collection.

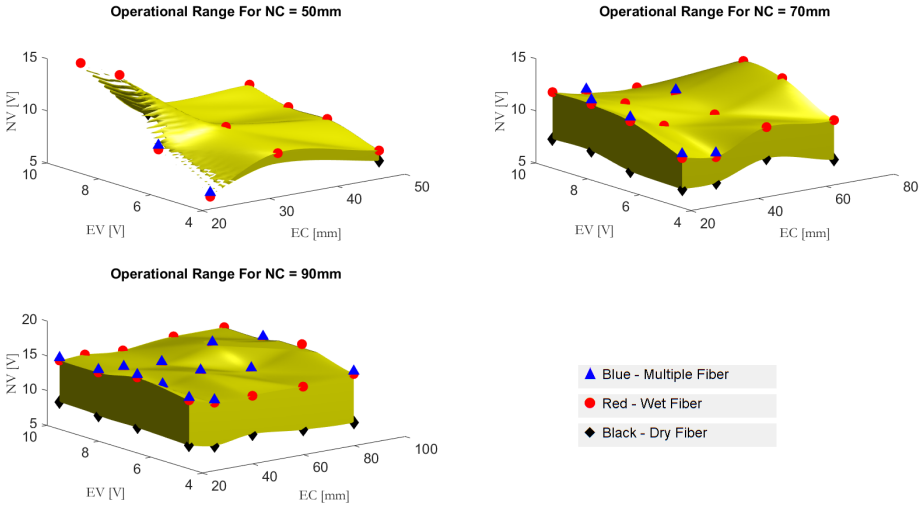

Fig. 6. Experimentally obtained stable fiber extrusion regimes in terms of nozzle voltage (NV) as a function of nozzle to collector distance(NC), focusing electrode voltage (EV), and focusing electrode to collector distance (EC).

After securing the steady nanofiber extrusion, electrostatic focusing parameters can be discussed. This is done in the following section.

6. Electrostatic Focusing Analysis

As previously stated, different electric field distributions inside of the electrospinning device lead to different fiber deposition patterns on the grounded

collector electrode. In terms of fiber focusing, obtained experimental data suggest, that the focusing effect of focusing electrodes is highest, when these electrodes are placed approximately in the middle of the distance from the nozzle to the collector electrode (NC). Separation (EE) and electric potential (EV) applied to the focusing electrodes are two parameters which need to be set together, to form a desired electric field inside the device. Increase in separation of focusing electrodes is effectively equal to lowering the electric potential on these electrodes. FEA analysis of a device with a pair of focusing electrodes was performed, and results of this numerical analysis are shown in Fig.7, where external electric field components along axes of the device are plotted.

Figure 7 shows that the $x-$ component of the electric field is non-zero, even without deflection electrodes operating along this axis. This is an effect of the low width of the focusing electrodes ($z-$ direction dimension) and a close presence of the nozzle (at high potential), and grounded collector. As an effect of this, the device becomes confining in both $-$ and $y-$ directions, where y direction external Coulomb forces are still about two orders of magnitude higher than those in $x-$ direction. Figure 7 also shows, that the $y-$ direction electric field is no longer linear as expected(Eqn.3). However, considering only the region close to the device axis ($z-$axis), where the fiber moves, it stays very close to linear. The steering effect of the electric fields was investigated further in order to establish optimal conditions.

Figure 8 shows three different electrospinning setups with electrostatic focusing are investigated in terms of focusing electric forces. Based solely on the electric field component in direction to the center plane of the device ($y-$axis), setup with lowest separation of these electrodes and highest applied electric potential (green/asterisk marked setup) would be chosen. This decision would be given by the fact that the highest electric field in this direction leads to the highest coulomb forces applied on the fiber by a set of focusing electrodes. However, limitations to the separation and potential on focusing electrodes exist. Firstly, limitation on the electric potential on focusing electrodes is introduced by the air breakdown voltage. As the space inside the device is in some setups limited,

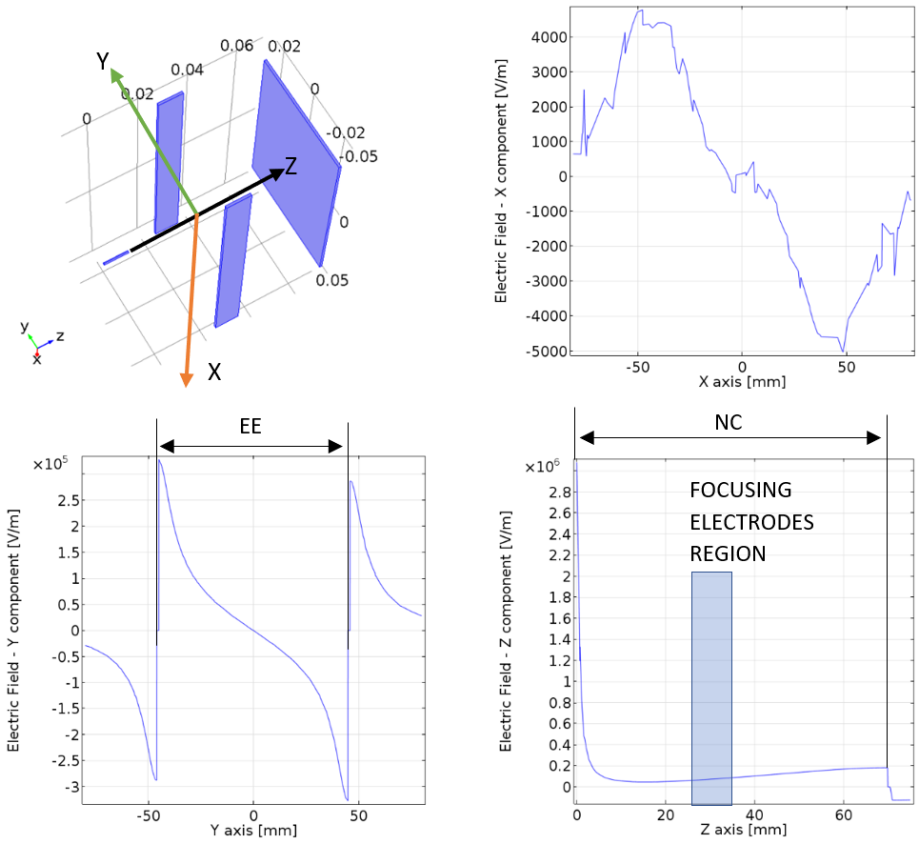

Fig. 7. FEA analysis of the electric field distribution in electrospinning device. Top-Left: electrospinning device layout; Top-Right: Electric field $x-$ component along the x axis between the focusing electrodes; Bottom-Left: Electric field $y-$ component along y axis, between the focusing electrodes; Bottom-Right: Electric field $z-$ component along the z axis of the design (from the nozzle to the collector electrode). Top-Right figure shows, that the electric field $x-$ component is non-zero along the $x-$ axis, even though there are no focusing electrodes on this axis.

it becomes difficult to keep safe distances between components of the device to prevent electric breakdown and potential damage on the apparatus. The air breakdown potential is even increased by increased humidity accumulated inside of the device from drying fiber. Secondly, and more importantly, if the electric potential along the axis of the device is plotted, for the case shown in

green/asterisk in Fig.8, it has a non-decreasing or even increasing character on some region along this axis. This leads to elimination of the electric field in $z-$ direction or even making it negative, what means that there is no or negative electric force along the axis of the device and so the fiber is not attracted to the collector electrode any longer, forcing it to collect on the walls of the device.

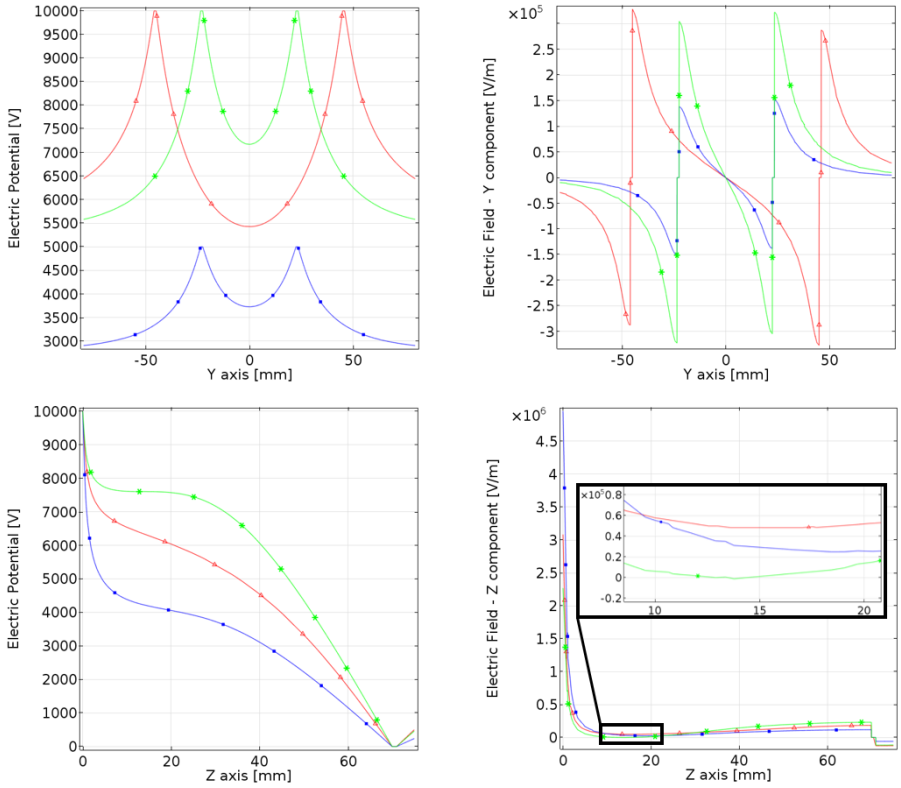

Fig. 8. FEA analysis of the electric potential and electric field distribution in the electrospinning device for three different setups of focusing electrodes. Fixed parameters: $NV = 10kV, NC = 70mm, NE = 30mm$; variable parameters: $EE = 90mm, EV = 10$ kV (red traces); $EE = 50mm, EV = 5$ kV (blue traces); $EE = 50mm, EV = 10$ kV. (green traces)

Set of figures from FEA analysis in Fig.9 show, how the electric potential distribution in horizontal plane and electric field lines (originating at the tip of the nozzle) change with increasing electric field in lateral direction and decreas-

ing in axial direction. Electric field lines are just a visualization of a vector field (Electric Field), and they represent a direction in which electric forces are acting on a charged particle in the particular location of this electric field. Even though they do not represent the exact trajectory of the fiber, as the initial acceleration of the fiber is not assumed nor the repulsion forces between the particles of the fiber or the mechanical forces, they give an insight on how the electrospinning device is influencing the fiber movement. Based on the field lines, four different electric field distribution regimes can be identified. These regimes labeled (A-D) are shown in Fig.9 The location of the two confining electrodes, shown in blue and red in Fig. 8, both lead to field distribution regime (B). Setup shown in green leads to distribution regime (D), as it doesn't allow fiber to pass between the focusing electrodes and form a deposit on a collector.

Existence of all four of these regimes was experimentally verified and the results are described in the following section.

7. Experimental Results

Among the four electric field distribution regimes, regimes B and C are the most important ones, and so this section will focus on these two. Except of these two electric field distribution regimes (Fig. 9), this section refers also to the fiber extrusion regimes shown in Fig. 6. Performed series of 120 experiments showed, that when the fiber extrusion was stable, and it was operated under field distribution regime B, it always collected in an almost circular deposition area within 1 cm in diameter (Fig. 10-Left). The size of this deposition region can be decreased by increase of focusing effect of electrodes increasing applied electric potential or decreasing the electrode separation, while remaining within the field distribution regime B. After reaching the field distribution regime C, the fiber is forced to a larger area of attraction and the deposition region increases in size and stretches in direction parallel to the focusing electrodes (Fig. 10-right).

If the electrospinning device is operated in an unstable fiber extrusion regime and it produces multiple fibers or disappearing/reappearing fibers, their behav-

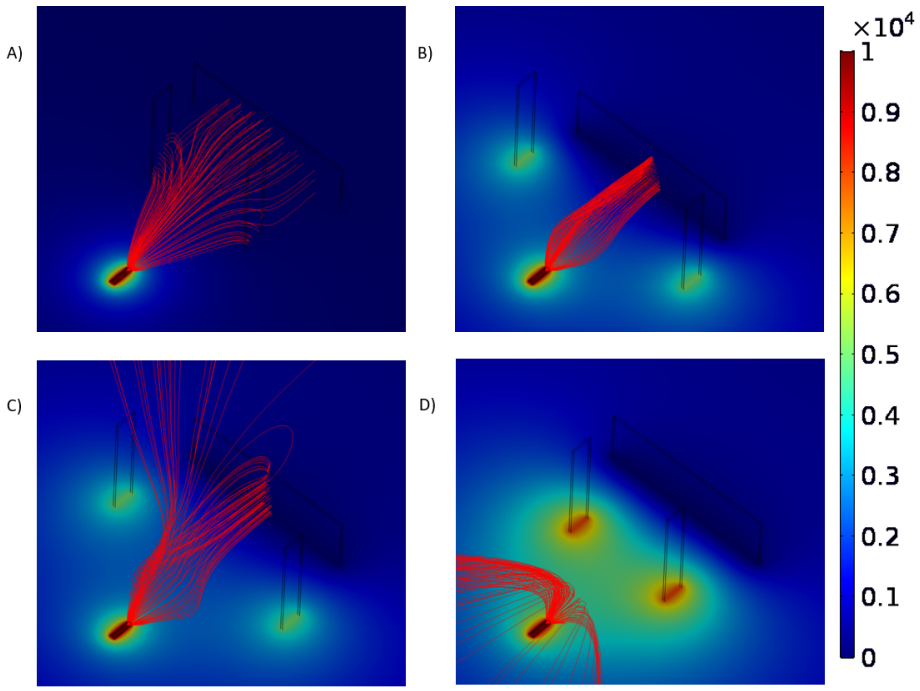

Fig. 9. FEA analysis of the electrospinning device with a pair of focusing electrodes. Electric potential distribution in horizontal plane and electric field lines originating at the tip of the nozzle are shown. Based on distribution of the electric field lines, four different electric field distribution regimes can be recognized: A-Attracting regime (fiber is at least partially collected on focusing electrodes); B-Focusing regime; C-Focusing and reverting regime (Some part of the fiber is collected outside of the collector electrode); D-Reverting regime (No fiber collection on collector, nor focusing electrodes)

ior is also influenced by the electrostatic focusing. Multiple fibers can be collected as a series of almost circular deposits for field distribution regime B, or a series of larger, non-circular, blown-up deposition regions for the field distribution regime C. These are shown in Fig. 11

After a fiber is created in the electrospinning device, it initially oscillates with higher amplitudes until it stabilizes. Therefore, disappearing and reappearing fiber from unstable extrusion regime oscillates much more than stably produced fiber. As this oscillatory motion of the fiber is compressed from sides by the

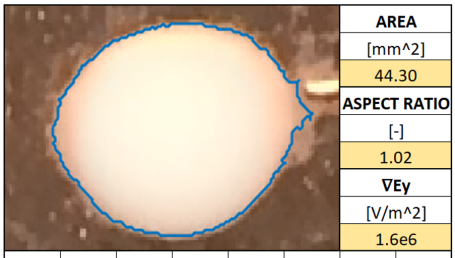

AREA [mm^2]	ASPECT RATIO [-]	∇Ey [V/m^2]
44.30	1.02	1.6e6

NC [mm]	NE [mm]	EE [mm]	NV [kV]	EV [kV]	FR [ml/hr]	CC [w%]	N [gage]
85	10	95	10	5	0.06	7.5	20

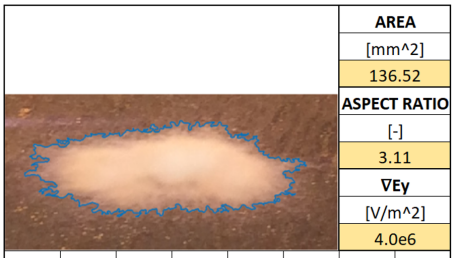

AREA [mm^2]	ASPECT RATIO [-]	∇Ey [V/m^2]
136.52	3.11	4.0e6

NC [mm]	NE [mm]	EE [mm]	NV [kV]	EV [kV]	FR [ml/hr]	CC [w%]	N [gage]
85	50	70	10	7.5	0.06	7.5	20

Fig. 10. PEO nanofiber deposit and its evaluation in MATLAB, with electrospinning parameters listed on the bottom of the figure. To the right from the experimental results are: area of fiber deposit, aspect ratio of the deposit(width/ height), and $\nabla E_y = \beta U_{DC}$ is a gradient of $y-$ component of the electric field along y axis between the focusing electrodes. Left: Stable fiber extrusion under electric field distribution regime B; Right: Stable fiber extrusion under electric field distribution regime B

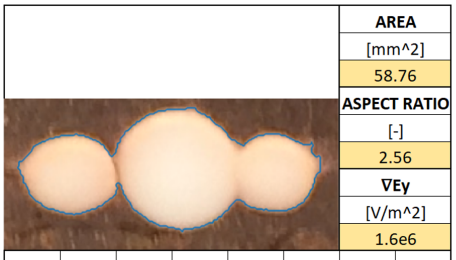

AREA [mm^2]	ASPECT RATIO [-]	∇Ey [V/m^2]
58.76	2.56	1.6e6

NC [mm]	NE [mm]	EE [mm]	NV [kV]	EV [kV]	FR [ml/hr]	CC [w%]	N [gage]
85	30	95	10	7.5	0.06	7.5	20

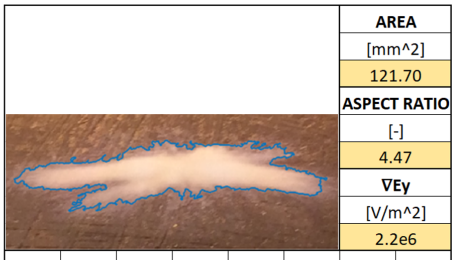

AREA [mm^2]	ASPECT RATIO [-]	∇Ey [V/m^2]
121.70	4.47	2.2e6

NC [mm]	NE [mm]	EE [mm]	NV [kV]	EV [kV]	FR [ml/hr]	CC [w%]	N [gage]
85	30	95	10	10	0.04	7.5	18

Fig. 11. PEO nanofiber deposit and its evaluation in MATLAB, with electrospinning parameters listed on the bottom of the figure. To the right from the experimental results are : area of fiber deposit, aspect ratio of the deposit(width/ height), and $\nabla E_y = \beta U_{DC}$ is a gradient of $y-$ component of the electric field along y axis between the focusing electrodes. Left: Unstable fiber extrusion (multiple fibers) under electric field distribution regime B; Right: Unstable fiber extrusion (multiple fibers) under electric field distribution regime B

electrostatic field created by focusing electrodes, the fiber deposits in an elliptical region if operated under field distribution regime B (Fig. 12-Left), or even more compressed line-like deposition region for stronger focusing electrostatic field in

field distribution regime C (Fig.12-Right)

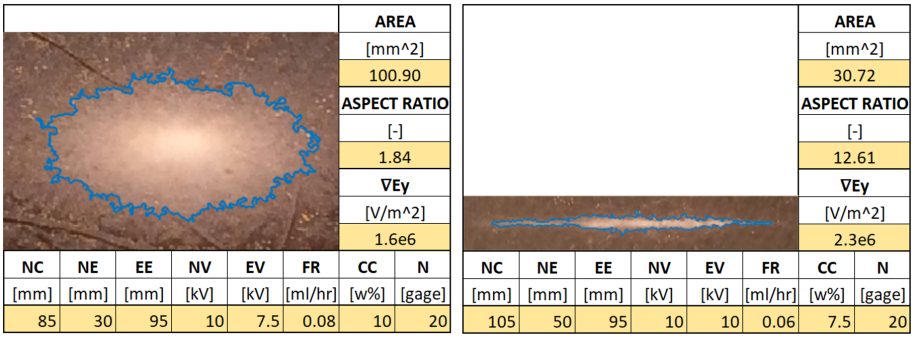

AREA [mm^2]	ASPECT RATIO [-]	∇Ey [V/m^2]
100.90	1.84	1.6e6

NC [mm]	NE [mm]	EE [mm]	NV [kV]	EV [kV]	FR [ml/hr]	CC [w%]	N [gage]
85	30	95	10	7.5	0.08	10	20

AREA [mm^2]	ASPECT RATIO [-]	∇Ey [V/m^2]
30.72	12.61	2.3e6

NC [mm]	NE [mm]	EE [mm]	NV [kV]	EV [kV]	FR [ml/hr]	CC [w%]	N [gage]
105	50	95	10	10	0.06	7.5	20

Fig. 12. PEO nanofiber deposit and its evaluation in MATLAB, with electrospinning parameters listed on the bottom of the figure. To the right from the experimental results are: area of fiber deposit, aspect ratio of the deposit (width/ height), and $\nabla E_y = \beta U_{DC}$ is a gradient of $y-$ component of the electric field along y axis between the focusing electrodes. Left: Unstable fiber extrusion (single fiber) under electric field distribution regime B; Right: Unstable fiber extrusion (single fiber) under electric field distribution regime B.

On the bottom of the series of figures Fig. 10 - 12, fiber deposit parameters (deposition area and aspect ratio) are shown together with the gradient of $y-$ component of the electric field along $y-$ axis in between the focusing electrodes. The electric field gradient is obtained from FEA analysis of the electrospinning device with given set of parameters. As shown in Fig.7, the electric field is linear in proximity to the axis of the device. This gradient of the $y-$ component electric field (βU_{DC} in Eqn.8) shows, that if kept at about $\beta U_{DC} \approx 1.6e6V/m^2$, it results in field distribution regime B. If increased to about $\beta U_{DC} = 2.2e6 - 4e6V/m^2$, it changes the distribution to regime C, and partial loss of the fiber occurs. In all experiments with electrostatic focusing, fiber deposition only in macroscopic scale was influenced. Even for runs with highest focusing potential, the fiber propagates in chaotic movement and deposits buckled. To achieve a periodic/quasi-periodic fiber movement or to straighten the fibers, electrodynamic focusing must be used.

8. Conclusions

Electrospinning device working parameters leading to a stable fiber extrusion were determined, where the stable fiber extrusion regime was defined as a continuous, single PEO polymer fiber extrusion that deposits dry on the collector electrode. Minimal axial component of the electric field ($z-$ direction) near the nozzle, required for electrospinning device to spin 5 wt% PEO, was found to be $E_{z\,min} = 1.6e6V/m$. In order for the device to collect fiber at the collector electrode,we found, this field component along the device axis may never decrease to zero or become negative. Possible explanation to this might be that the mass of the fiber and therefore its inertia is very low, what in combination with nonzero lateral component of the electric field leads to a deflection of the fiber from the axis of the device in such extent that it doesn‘t collect on the collector electrode.

In terms of fiber focusing, electrostatic focusing capabilities and limitations, together with four electric field distribution regimes were determined and experimentally verified. A confining, lateral direction electric field gradient for effective fiber steering with no fiber loss, was found to be on interval of $\beta U_{DC} = [1.6e^6V/m^2,\ 2.2e6V/m^2]$. Above the upper boundary of this electric field gradient, fiber was partially dispersed and only partially collected on the collector electrode. If increased even further, fiber travel was reversed and no collection on the collector electrode was observed.

Acknowledgments

This material is based upon work supported by the National Science Foundation under Grant No. 1462752

References

[1] D. H. Reneker, A. L. Yarin, Electrospinning jets and polymer nanofibers, Polymer 49 (10) (2008) 2387 – 2425. doi:10.1016/j.polymer.2008.02.002.

[2] N. Bhardwaj, S. C. Kundu, Electrospinning: A fascinating fiber fabrication technique, Biotechnology Advances 28 (2010) 325 – 347. doi:10.1016/j.biotechadv.2010.01.004.

[3] B. Sundaray, V. Subramanian, T. Natarajan, R. Xiang, C. Chang, W. Fann, Electrospinning of continuous aligned polymer fibers, Applied physics letters 84 (7) (2004) 1222–1224.

[4] J. Doshi, D. H. Reneker, Electrospinning process and applications of electrospun fibers, Journal of Electrostatics 35 (2) (1995) 151 – 160. doi:10.1016/0304-3886(95)00041-8.

[5] H. Yuan, Q. Zhou, Y. Zhang, 6 - improving fiber alignment during electrospinning, in: M. Afshari (Ed.), Electrospun Nanofibers, Woodhead Publishing Series in Textiles, Woodhead Publishing, 2017, pp. 125 – 147. doi:10.1016/B978-0-08-100907-9.00006-4.

[6] V. Beachley, E. Katsanevakis, N. Zhang, X. Wen, Highly Aligned Polymer Nanofiber Structures: Fabrication and Applications in Tissue Engineering, 2012, pp. 171–212. doi:10.1007/12_2011_141.

[7] M. M. L. Arras, C. Grasl, H. Bergmeister, H. Schima, Electrospinning of aligned fibers with adjustable orientation using auxiliary electrodes, Science and Technology of Advanced Materials 13 (3). doi:10.1088/1468-6996/13/3/035008.

[8] P. Kiselev, J. Rosell-Llompart, Highly aligned electrospun nanofibers by elimination of the whipping motion, Journal of Applied Polymer Science 125 (2012) 2433–2441. doi:10.1002/app.36519.

[9] X. Cui, L. Li, F. Xu, Controlled assembly of poly(vinyl pyrrolidone) fibers throughanelectric-field-assisted electrospinning method, Applied Physics A 103 (1) (2011) 167–172. doi:10.1007/s00339-010-6036-y.

[10] C. Grasl, M. Arras, M. Stoiber, H. Bergmeister, H. Schima, Electrodynamic control of the nanofiber alignment during electrospinning, Applied Physics Letters 102 (5). doi:10.1063/1.4790632.

[11] L. M. Bellan, H. G. Craighead, Control of an electrospinning jet using electric focusing and jet-steering fields, Journal of Vacuum Science & Technology B: Microelectronics and Nanometer Structures 24 (6). doi:10.1116/1.2363403.

[12] M. Arras, Macro-and Microscopical Alignment of Electrospun Fibres with Possible Use for Vascular Grafts: Experiment and Simulation, 2010. doi:10.13140/RG.2.1.5039.6004.

[13] W. Hwang, C. Pang, H. Chae, Fabrication of aligned nanofibers by electric-field-controlled electrospinning: insulating-block method, Nanotechnology 27 (43) (2016) 435301.

[14] W. Paul, Electromagnetic traps for charged and neutral particles, Rev. Mod. Phys. 62 (1990) 531–540. doi:10.1103/RevModPhys.62.531.

[15] R. Coisson, G. Vernizzi, X. Yang, Mathieu functions and numerical solutions of the mathieu equation, 2009, pp. 3–10. doi:10.1109/OSSC.2009.5416839.

[16] L. Ng, R. Rand, Bifurcations in a mathieu equation with cubic nonlinearities, Chaos, Solitons and Fractals 14 (2) (2002) 173 – 181. doi:10.1016/S0960-0779(01)00226-0.

[17] G. Box, D. Behnken, Some new three level designs for the study of quantitative variables, Technometrics 2 (4) (1960) 455–475. doi:10.1080/00401706.1960.10489912.

[18] A. Haider, S. Haider, I.-K. Kang, A comprehensive review summarizing the effect of electrospinning parameters and potential applications of nanofibers in biomedical and biotechnology, Arabian Journal of Chemistrydoi:10.1016/j.arabjc.2015.11.015.

[19] V. Beachley, X. Wen, Effect of electrospinning parameters on the nanofiber diameter and length, Materials Science and Engineering: C 29 (3) (2009) 663 – 668. doi:10.1016/j.msec.2008.10.037.

[20] Z. Li, C. Wang, One-dimensional nanostructures electrospinning technique and unique nanofibers, 2013. doi:10.1007/978-3-642-36427-3-2.